POLSKA AKADEMIA NAUK

M&S

A NEW APPROACH TO WATER COOLING OF PHOTOVOLTAIC PANELS WITH A TRACKING SYSTEM

Kamil Płachta, Janusz Mroczka, Mariusz Ostrowski

Wroclaw University of Technology, Faculty of Microsystem Electronics and Photonics, Chair of Electronic and Photonic Metrology, Bolesława Prusa 53/55, 50-317 Wrocław, Poland (✉ kamil.plachta@pwr.edu.pl, janusz.mroczka@pwr.wroc.pl, mariusz.ostrowski@pwr.edu.pl)

Abstract

The article presents a water-cooling system for photovoltaic (PV) modules using a two-axis tracking system that tracks the apparent position of the Sun on the celestial sphere. The cooling system consists of 150 adjustable spray nozzles that cool the bottom layer of PV modules. The refrigerant is water taken from a tank with a capacity of 7 m^3. A water recovery system reduces its consumption with efficiency of approximately 90%. The experimental setup consists of a full-size photovoltaic installation made of 10 modules with an output power of 3.5 kWp combined with a tracking system. The article presents an analysis of the cooling system efficiency in various meteorological conditions. Measurements of energy production were performed in the annual cycle using three different types of photovoltaic installations: stationary, two-axis tracking system and two-axis tracking system combined with the cooling system.

Keywords: photovoltaic system, cooling system, solar tracking system.

1. Introduction

Most of solar radiation absorbed by *photovoltaic* (PV) cells is converted into heat, and only 15–20% is converted into electricity. Technologies such as half-cut or *heterojunction solar cells* (HJT) help to limit the temperature rise of photovoltaic panels. The effectiveness of applied solutions can be judged by the temperature coefficient of power (γ), which determines the decrease in PV module efficiency with a temperature increase of 1°C. Usually, the value of γ factor does not exceed 0.42%/°C. In the case of PV module made in half-cut or HJT technology, the value of the temperature coefficient of power is in the range of 0.25–0.37%/°C, for the tested PV modules is equal to 0.35%/°C. Dupeyrat *et al.* using a commercial c-Si PV cell performed measurements of spectral reflection and spectral response of the tested PV cell. About 90% of solar radiation is absorbed by the photovoltaic cells [1]. Therefore, reducing the temperature of a PV module can significantly increase efficiency. Cooling techniques for photovoltaic modules are divided into passive and active methods [2]. The passive methods use water or air to cool

photovoltaic surface, whereas, active methods are those that use energy to cool PV modules, *e.g.* the Peltier effect [3]. Currently, there is a dynamic development of co-generation components such as *PV-thermal collectors* (PVTs). The solution uses photovoltaic cells and an absorber that removes excess heat. PVT modules do not have a selective absorber and thermal insulation as good as typical solar collectors, which causes a higher heat loss. Therefore, the obtained medium temperature is lower. Despite that, it is one of the most effective solutions for converting solar energy into electricity, therefore many studies and measurements have been carried out theoretically and experimentally [4–6]. Herrando M. *et al.* developed a method for modelling the efficiency of conversion of solar energy to electricity by combined cooling, heating and power systems based on hybrid PVT collectors [7].

Nomenclature

A_{PV}	– surface area of PV module [m²]	
c_g	– specific heat capacity of glass [J/(kg·K)]	
c_w	– specific heat capacity of water [J/(kg·K)]	
G_T	– solar radiation power density [W/m²]	
$G_{T,NOCT}$	– solar radiation intensity in NOCT [W/m²]	
I	– photovoltaic cell current [A]	
I_{PH}	– photocurrent generated in the PV cell [A]	
I_D	– diode current [A]	
I_{D0}	– dark current of diode [A]	
I_S	– solar irradiance incident on PV surface [W/m²]	
I_{SH}	– shunt resistance current [A]	
I_{SC}	– short-circuit current [A]	
I_L	– load current [A]	
J_0	– temperature coefficient [A/K]	
$\dot{m}_w$	– mass of flow water [kg]	
m_g	– mass of glass [kg]	

P_{max}	– maximum power generated from PV modules [W]
R_S	– series resistance [Ω]
t	– cooling time [s]
$t_{A,NOCT}$	– ambient temperature in NOCT conditions [°C]
t_{PV}	– cell temperature [°C]
$t_{PV,STC}$	– temperature of PV cell in STC conditions [°C]
$t_{PV,NOCT}$	– temperature of PV cell in NOCT cond. [°C]
U_L	– load voltage [V]
$\dot{V}$	– volume of flow rate [m/s]
α_p	– temperature power factor [%/°C]
α_q	– diode quality factor
ρ_g	– glass density [kg/m³]
ρ_w	– water density [kg/m³]
η_{PV}	– efficiency of photovoltaic module [%]
η_{STC}	– efficiency of photovoltaic module in STC cond. [%]
ξ	– nominal efficiency of photovoltaic module [%]

On the other hand, Vallati A. *et al.* studied the efficiency of a thermal system composed of a heat pump coupled with PV-thermal collectors [8]. Another solution to increase efficiency of solar energy conversion into electricity is the use of PVT collectors with solar concentrator systems [9–11]. A solar concentrator increases the value of solar radiation intensity falling onto a photovoltaic surface, but at the same time increases the temperature of PV modules. In the case of photovoltaic thermal collectors, the increase in the temperature power factor is limited by the cooling system. However, the solution is very rarely used commercially because the solar radiation concentrator should be combined with a tracking system which eliminates the shading and masking effect caused by the concentrator mirrors [12]. Therefore, the cooling systems are most often used in photovoltaic systems installed on the ground. The article presents the solution for a cooling system adapted to a two-axis tracking system which changes the spatial orientation of the PV system [13–15].

2. Effect of overheating on the efficiency of a PV module

In the mathematical analysis of a photovoltaic module a single-diode model was used. A single-diode model of an ideal PV cell contains a parallel connection of the power source and diode. For a better representation of the actual operating conditions of the photovoltaic cell, series resistance (R_s) and shunt resistance (R_{SH}) are also taken into account. The single-diode model of a PV cell is described by the equation:

$$I = I_{PH} - I_D - I_{SH}, \tag{1}$$

where: I – photovoltaic cell current, I_{PH} – photocurrent generated in the PV cell, I_D – diode current, I_{SH} – shunt resistance current.

The value of the I_{PH} depends on the intensity of solar radiation and the temperature of the photovoltaic module. The value of I_{PH} is described by following equation:

$$I_{PH} = I_{SC} \left(\frac{G_T}{1000} \right) + J_0 (t_{PV} - t_{PV,STC}), \tag{2}$$

where: I_{SC} – short-circuit current, G_T – solar radiation power density, J_0 – temperature coefficient, t_{PV} – cell temperature, $t_{PV,STC}$ – cell temperature in *standard test conditions* (STC).

The value of the diode current (I_D) is determined as follows:

$$I_D = I_0 \left[\exp \left(\frac{q \, (U_L + R_S I_L)}{\alpha_q k_B t_{PV}} \right) - 1 \right], \tag{3}$$

where: $q = 1.602 \cdot 10^{-19}$ [C], U_L – load voltage, R_S – series resistance, I_L – load current, α_q – diode quality factor, k_B – Boltzmann's constant $1.38 \cdot 10^{-23}$ [J/K]. The relationship determines the value of the current I_0 the:

$$I_0 = I_{D0} \left(\frac{t_{PV}}{t_{PV,STC}} \right)^3 \exp \left[\frac{q E_q}{\alpha_q k_B} \left(\frac{1}{t_{PV,STC}} - \frac{1}{t_{PV}} \right) \right], \tag{4}$$

where: I_{D0} – the "dark" current of diode. Substituting the presented mathematical dependencies (2)–(4), for the (1) the mathematical model has been obtained of a photovoltaic cell, which was used in the current-voltage and output power analysis:

$$I = I_{SC} \left(\frac{G_0}{1000} \right) + J_0 (t_{PV} - t_{PV,STC}) - I_0 \left[\exp \left(\frac{q \, (U_L + R_S I)}{\alpha_q k_B t_{PV}} \right) - 1 \right] - \frac{U + R_S I}{R_{SH}}. \tag{5}$$

In the case of a good quality photovoltaic cell, for the value of $R_S \cdot R_{SH}^{-1} \ll 1$, it can be assumed that the value of the I_{SC} is approximately equal to the value of I_{PH}. Assuming that $I_L = 0$ and $U = U_{OC}$, *i.e.* when the electrodes of the cell are not connected to each other, the equation of the open circuit voltage (U_{OC}) is obtained:

$$U_{OC} = \frac{k_B t_{PV}}{q} \cdot \ln \left(1 + \frac{I_{SC}}{I_0} \right). \tag{6}$$

Based on the presented (1)–(6), it can be concluded that the efficiency of a photovoltaic module is strongly related to its temperature. Using the single-diode model and technical parameters of the Q.PEAK DUO-G8 [16] photovoltaic module, the power-voltage P(V) characteristics (Fig. 1) were obtained for four different temperature values: 0°C, 25°C, 50°C and 75°C, which is presented below.
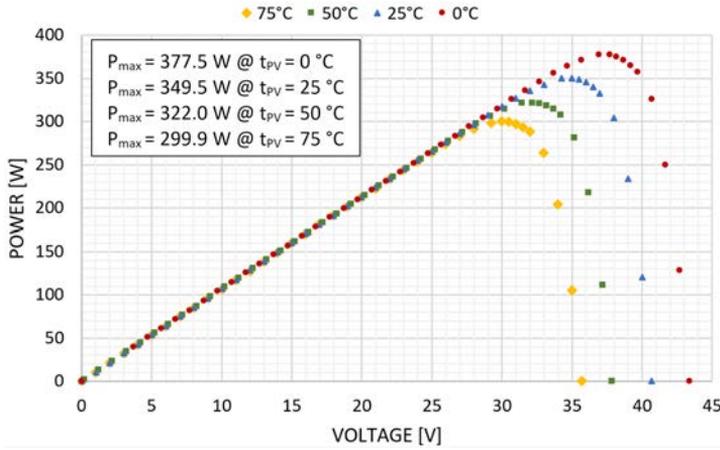
Fig. 1. The power-voltage characteristics of Q.PEAK DUO-G8 PV cell as a function of temperature
for 0°C, 25°C, 50°C and 75°C.

The power-voltage characteristics are the relation between the electrical power output and
the voltage output depending on the temperature of the PV module. An increase in the temperature
of the photovoltaic module causes a decrease in the temperature coefficient of voltage (β) by
0.27%/°C and an increase in temperature coefficient of current (α) by 0.04%/°C. As a result,
an increase in temperature of PV by 1°C increases the value of the temperature coefficient
of power (γ) by 0.35%/°C [16]. To verify the given parameters can be used solar simulator [17].
The amount of electricity produced by a PV system depends on the temperature of the PV
modules. An increase in temperature of 25°C reduces the output power of the photovoltaic module
by 9% (ground installation) and 18% (rooftop installation) [18, 19]. Moreover, the degradation
of PV modules and their subsequent loss of performance has a serious impact on the energy
produced. The changes in parameters during the time operation of PV panels can be determined
using algorithms that use the value of the output voltage and current [20]. In order to increase
the amount of electricity produced by a photovoltaic system, the temperature of the photovoltaic
panels should be maintained in conditions similar to the *normal operating cell temperature*
conditions (NOCT).

In the analysis of output power of a PV module in relation to its temperature, there can be
applied a simplified formula that uses the values of ambient temperature, solar radiation intensity
and parameters in NOCT conditions [21]:

$$t_{\mathrm{PV}} = t_A + \left(t_{\mathrm{PV,NOCT}} - t_{A,NOCT}\right)\left(\frac{G_T}{G_{T,\mathrm{NOCT}}}\right) \tag{7}$$

where: $t_{\mathrm{PV,NOCT}}$ − temperature of the photovoltaic cell in NOCT conditions, $t_{A,\mathrm{NOCT}}$ − ambient
temperature in NOCT conditions, $G_{T,\mathrm{NOCT}}$ − solar radiation intensity in NOCT conditions.
Equation (7) does not take into account the temperature power factor and temperature under
standard test conditions. For the most accurate results of simulation, there was used a relationship
proposed by Homer, who uses the given parameters in NOCT and STC conditions [22]:

$$t_{\mathrm{PV}} = \frac{t_A + \left(t_{\mathrm{PV,NOCT}} - t_{A,\mathrm{NOCT}}\right)\left(\frac{G_T}{G_{T,\mathrm{NOCT}}}\right)\left[1 - \frac{\eta_{\mathrm{STC}}\left(1-\alpha t_{\mathrm{PV,STC}}\right)}{\tau\,\alpha_{\mathrm{PV}}}\right]}{1 + \left(t_{\mathrm{PV,NOCT}} - t_{A,\mathrm{NOCT}}\right)\left(\frac{G_T}{G_{T,NOCT}}\right)\left(\frac{\gamma\,\eta_{\mathrm{STC}}}{\tau\,\alpha_{\mathrm{PV}}}\right)}, \tag{8}$$

where: $t_{PV,STC}$ – cell temperature in standard test conditions, γ – temperature coefficient of power, η_{STC} – efficiency of PV module in STC conditions, $\tau\alpha_{PV}$ – product of transmittance and absorptivity. In the mathematical analysis, there should be included the parameters that characterize a particular PV module. This is important to obtain reliable results.

3. Experimental setup

The temperature of photovoltaic cell has a significant impact on the amount of electricity produced. PV modules placed on a tracking system reach a temperature of 52–54°C on a cloudless, sunny day. According to datasheet of the PV module [16], the output power of the PV system should be 7.6 percentage points less than the nominal output power. The measurement results made with the SOFAR inverter (Fig. 2) indicate that the maximum output power on a sunny, cloudless day was 2.8 kW, instead of the theoretical 3.3 kW. On the next day, the output power was measured during the day with temporary overcast. Cloudiness lowered the temperature of the photovoltaic modules, which temporarily increased the output power to the nominal value after the cloud has passed. The increase of PV module temperature on sunny, cloudless day caused a decrease in produced power at the level of 13.4% in relation to the nominal value output power.
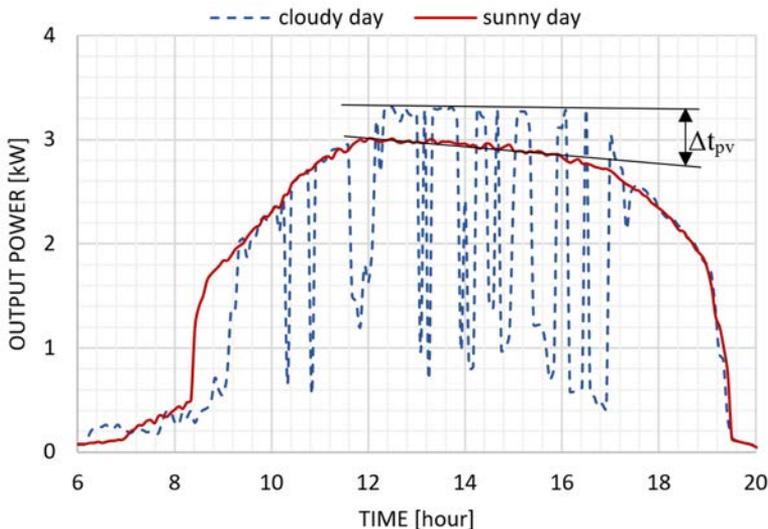

Fig. 2. Output power of the experimental setup on a temporary overcast and sunny day.

The experimental setup was made to study the effect of cooling on the output power of photovoltaic modules. The experimental setup consists of two-axis tracking system adapted to photovoltaic installation comprising 10 modules with the total power equal to 3.5 kWp and combined with a SOFAR inverter with an output power of 3.3 kW (Table 1). The tracking system allows to change the position of PV modules from 0° to 235° in the horizontal direction, and 0°–75° in the vertical direction. The apparent position of the Sun on the celestial sphere is determined by the developed tracking controller [23].

The cooling system consists of spray nozzles, an electronic driver and a high-pressure water pump with a tank. The block diagram of the presented solution is shown in Fig. 3.

Table 1. Electrical and physical characteristics of the applied photovoltaic module.

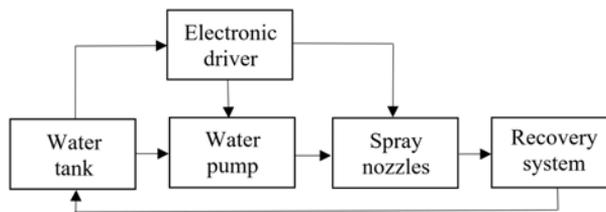| Electrical characteristics			Temperature coefficients	
Model no.	Q.PEAK DUO-G8		Temperature coefficient of current α	$+0.04\% \cdot {}^\circ\mathrm{C}^{-1}$
Power at maximum power point P_{MPP}		350 W	Temperature coefficient of voltage β	$-0.27\% \cdot {}^\circ\mathrm{C}^{-1}$
Open circuit voltage V_{OC}		40.7 V	Temperature coefficient of power γ	$-0.35\% \cdot {}^\circ\mathrm{C}^{-1}$
Short circuit current I_{SC}		10.74 A	Physical characteristics	
Voltage at maximum power point V_{MPP}		34.24 V	Cell type	Monocrystalline silicon
Current at maximum power point I_{MPP}		10.22 A	Photovoltaic system	10 modules
Panel efficiency η		19.5%	Inverter SOFAR	3300 W

Fig. 3. Elements of the cooling system.

The cooling system uses 150 nozzles located on the tracker frame. The nozzles spray a thin layer of water onto the bottom layer of PV modules. Each of them cooled by 15 nozzles arranged in 3 rows of 5 pieces. The power of water stream of each nozzle is regulated by changing the opening angle in the range from 10° to 140°. The distance between the photovoltaic module and the nozzles is adjustable in the range of 10–50 cm, which allows for 94% coverage of the photovoltaic surface. The cooling system uses an underground tank with the capacity of 7 m^3, to which rainwater is directed. A high-pressure pump with a power of 1320 W, a water flow of 120 l/min and a water stream height of 78 m is used to ensure adequate water pressure in the cooling system.

The cooling system is controlled by an electronic driver which processes data from temperature sensors resulting in turning on and off the spray nozzles. The temperature measurement is performed for the four outermost photovoltaic panels which are located on the left and right side of the tracking system. The temperature of each solar module is measured at four points. It is not necessary to measure the temperature of each module because the tracking system eliminates the shading effect. The driver of the cooling system allows to control the spraying with a fixed time period or temperature hysteresis. In the first case, the user specifies the time to turn on and off the nozzles of the cooling system. In the second, the electronic driver automatically controls the nozzles based on the temperature value of the photovoltaic modules. It is also possible to trigger the system manually, but the most effective solution is to work in a specific temperature range. The measuring system starts with measuring the temperature of the photovoltaic panels. If their temperature is higher than the set maximum value (t_{max}), the water jets cool down the PV module until the temperature reaches the set minimum value (t_{min}). If the temperature of the photovoltaic module is lower than the set value t_{min}, the device is deactivated.

4. Energy balance model and experimental results

The temperature value of the PV module was calculated with the energy balance of the cooling medium (Q_{gcw}) and the thermal energy of the photovoltaic panel (Q_{dPV}):

$$Q_{gcw} = Q_{dPV}, \tag{9}$$

$$\dot{m}_w \cdot t \cdot c_w \cdot \Delta T_w = m_g \cdot c_g \cdot \Delta T_g, \tag{10}$$

where: $\dot{m}_w$ – mass of flow water, t – cooling time, c_w – specific heat capacity of water, ΔT_w – rise of water temperature, m_g – mass of the glass, c_g – specific heat capacity of glass, ΔT_g – temperature change of the glass due to water cooling. The mass of the flow water (m_w) and the mass of glass (m_g) can be calculated as:

$$\dot{m}_w = \rho_w \cdot \dot{V}, \tag{11}$$

$$m_g = \rho_g \cdot A_{PV} \cdot x_g \tag{12}$$

where: ρ_w – water density, $\dot{V}$ – volume of flow rate, ρ_g – glass density, A_{PV} – surface area of the PV module, x_g – thickness of the glass covering the photovoltaic module. By transforming (10) and using (11) and (12), the cooling time of PV module is equal to:

$$t = \frac{\rho_g \cdot A_g \cdot x_g \cdot c_g \cdot \Delta T_g}{\rho_w \cdot \dot{V} \cdot c_w \cdot \Delta T_w}. \tag{13}$$

Photovoltaic panels should operate at a temperature close to temperature in standard test conditions. Sudden and permanent changes of temperature amplitude may affect the lifetime of the PV module. The temperature change was measured after turning on the cooling system (Fig. 4) and after turning it off (Fig. 5). The aim of the study was to determine the dynamics of the temperature change in order to select the appropriate operating range of the photovoltaic module. The test was performed under the following conditions: external temperature 32.4°C, wind speed not exceeding 4 m/s, temperature of water: 16.2°C. The results of average temperature measurements for four measuring points are presented in the figures below.
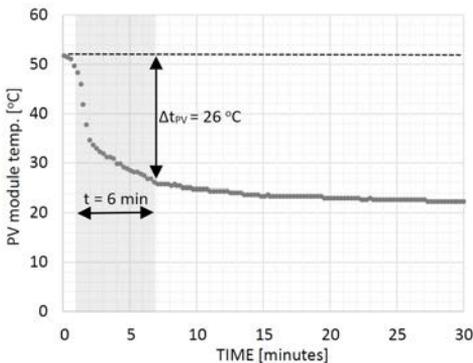

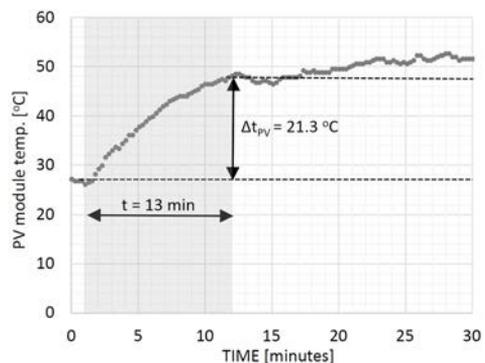Fig. 4. Temperature change of the PV module after turning on the cooling system.

Fig. 5. The temperature change of the PV module after turning off the cooling system.

The obtained results show high efficiency of the presented cooling system. Ninety seconds after starting the cooling system (Fig. 4), the temperature of the PV modules dropped from

51.3°C to 35.1°C. During the next 5 minutes, the rate of decline decreased, and the module temperature reached 25°C. This value corresponds to the STC conditions in which the solar modules are tested. After 7 minutes from the start, the temperature change becomes slower – during the next 23 minutes of measurements the temperature decreased by 3°C. Taking into account the obtained results, the cooling system should operate in the temperature range from 25°C to 35°C. It is a compromise between the consumption of water and high temperature amplitude of the photovoltaic cell. Also, the temperature change of the photovoltaic module was measured after the cooling system was turned off. The measurement was performed at the temperature of 31.3°C and the water temperature 17.1°C. The cooling system was turned off (Fig. 5) one minute after the start of the measurements – the temperature of photovoltaic module remained in the range of 27–29°C. Turning off the cooling system caused a sharp increase in the temperature of the PV module. After 5 minutes the temperature increased by 10°C. After another 6 minutes, the solar module has reached a temperature equal to 49°C. Next, the temperature increase slowed down and after another 10 minutes, the photovoltaic module reached its nominal value.

5. Cooling system efficiency

The output power was measured on a sunny, cloudless day. The experimental setup of 10 PV modules has been divided and half of them worked with a cooling system which kept the module temperature in the range of 27°C to 29°C (solid line), while the other half did not use the cooling system (dotted line). All tested modules used a two-axis tracking system.
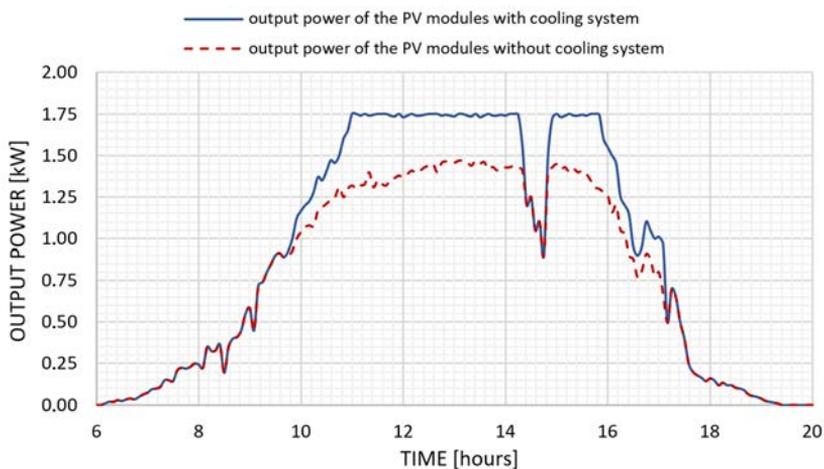

Fig. 6. Output power of the PV modules with and without the cooling system.

The measurement results showed that the photovoltaic panels merged with the cooling system worked at the maximum output power. In the case of photovoltaic modules that did not use the cooling system, the output power reached the highest value of 1.45 kW, which is 83% of its maximum value. To better compare the results of both solutions, there was used the efficiency factor η_{PV}, which can be calculated as:

$$\eta_{PV} = \frac{P_{max}}{I_s \cdot A_{PV}} \cdot 100\%, \tag{14}$$

where: P_{max} – maximum power generated from the photovoltaic modules, I_s – solar irradiance incident on photovoltaic surface and A_{PV} – surface area of the panels. The factor ξ determines the value of nominal efficiency of photovoltaic module:

$$\xi = \frac{\eta_{PV}}{\eta} \cdot 100\%. \tag{15}$$

The results presented in the diagram (Figs. 7 and 8) show the value of nominal efficiency of the PV module. The measurements were taken in the time period (11 am–2 pm), which is characterized by an average value of solar radiation intensity equal to 981 W/m^2, average ambient temperature of 34.8°C and a clear sky.
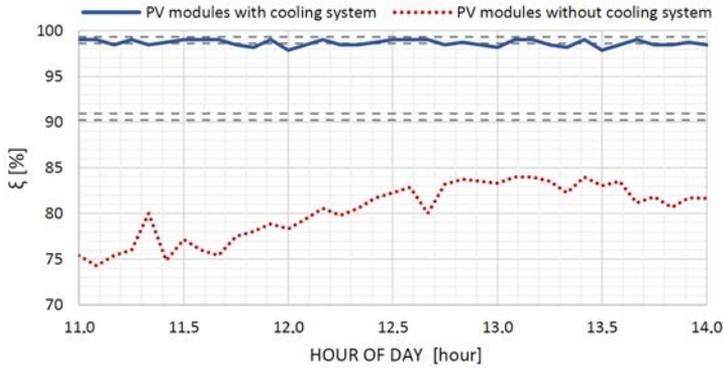

Fig. 7. Value of the nominal efficiency of PV modules with the cooling system ($t_{PV} = 27-29°C$)
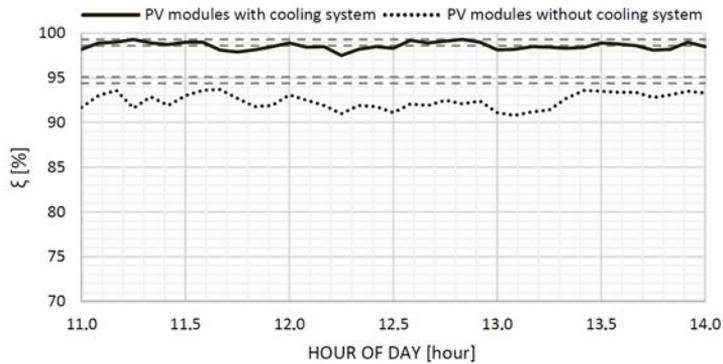and without the cooling system ($t_{PV} = 51-53°C$).

Fig. 8. Value of the nominal efficiency of PV modules with the cooling system ($t_{PV} = 27-29°C$)
and without the cooling system ($t_{PV} = 33-35°C$).

Using a cooling system provides 97.9–99.0% value of nominal efficiency of PV the module on a sunny cloudless day (Fig. 7). The horizontal lines mark the theoretical range in which coefficient ξ should be placed. The use of the cooling system ensures the output power of the PV modules comparable to that achieved in STC conditions. In the case of the photovoltaic panels that did not use the cooling system, their output power was lower than theoretical. The largest difference was 15.9% and the lowest 6.2%, while the average value in the measured range was

lower by 9.9%. Then, the nominal efficiency of the photovoltaic panels, whose temperature was maintained in the range of 27–29°C and 33–35°C by the cooling system (Fig. 8), was measured. The measurements were taken between 11 am–2 pm, with an average value of solar radiation intensity of 965 W/m^2, average ambient temperature equal to 33.2°C and clear sky. Thew application of the cooling system reduces the value of the change in the temperature amplitude of the photovoltaic panels. In the case of temperature in the range of 27–29°C (Fig. 7), the results are comparable with those presented in Fig. 8. The smallest value of coefficient ξ is equal to 97.5% and the highest is 99.2%, (average 98.6%). These values are in accordance with the temperature range determined on the basis of the PV module datasheet. In the case of the operating temperature of the PV modules in the range of 33–35°C, the average value of the ξ is 92.4%, which is 1.9 percentage points below the lower theoretical range. Whereas the maximum value of ξ factor is 93.7%, the minimum is equal to 90.8%. The use of the cooling system maintains the temperature of the PV modules in a set range, which is comparable with the data in STC. The absence of the cooling system causes the PV panels to operate more than 10% below the conditions specified in the standard test conditions. It is worth noting that measurements were made on PV modules that were not located on the roof. In that case, the difference between measured and theoretical value would be even greater.

The analysis of energy produced by photovoltaic system (10 PV modules cooperating with a 3.3 kW inverter) in various meteorological conditions was performed for three configurations:
1. Stationary (steel frame inclined at angle of 37°and facing south).
2. A two-axis tracking system (tracks the apparent position of the Sun on the celestial sphere).
3. A two-axis tracking and a cooling system (tracks the apparent Sun position and maintains the PV module temperature at a set level).

The analysis of energy production was performed on the basis of the measurement results obtained in the twelve-month period from January to December (Fig. 9).
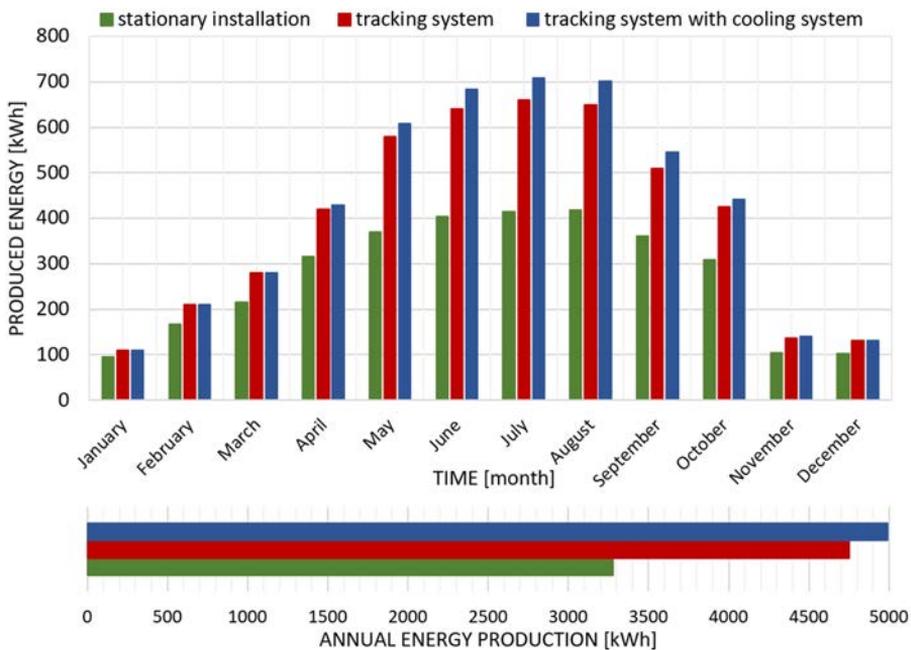

Fig. 9. Monthly energy production [kWh] by photovoltaic installation in stationary, tracking and tracking with cooling systems.

The stationary PV installation facing south and inclined at angle of 37° produced 3.28 MWh in 12 months. At the same time, the application of the tracking system increased the production to 4.75 MWh. It is an average increase of 45% compared to a stationary PV system. The use of the cooling system with tracking system provided energy production of 4.99 MWh in tested period, which is a 5% increase compared to the tracking system alone. The tracking system in the winter months (November-March) provided a 26.4% increase, whereas in the summer months (May – September) energy production was increased by 57.5% compared to stationary PV modules. The application of the cooling system increased energy produced by 5% compared to the modules using the tracking system only. During the five warmest months (May – September), the cooling system increased the amount of energy produced by 209.5 kWh, compared to the standard tracking system, which is equal to a 6.9% increase. Whereas, in the months with the highest value of solar radiation intensity and average ambient temperature (July – August), an increase in energy production equalled 7.7%.

Water consumption by the cooling system is proportional to the value of solar radiation intensity in a tested month. The cooling system was not used during the winter months with low ambient temperatures. In months with the highest average ambient temperature (July, August), the cooling system used almost twice as much water as compared to June and September. Detailed water consumption for each month is presented in Table 2.

Table 2. Water consumption by the cooling system depending on the month.

Month		April	May	June	July	August	September	October	Total
Water consumption	[dm^3]	6075	10725	33263	56115	61950	35288	2150	205566
	[m^3]	6	11	33	56	62	35	22	206

Despite the high water consumption (206 m^3), the operating costs of the cooling system is insignificant. The use of a water recovery system with an external tank (7 m^3) allowed for recovery of almost 90% of water. Moreover, the water tank is supplied with rainwater, which further reduces the cost of operation the cooling system.

6. Conclusions

The presented cooling system increases the efficiency of the photovoltaic system, ensures the energy production with a power comparable to that in STC conditions. The analysis of temperature change of photovoltaic modules cooperating with the cooling system showed that the PV module temperature should be maintained in the range of 25°C to 27°C.

The photovoltaic installation with an output power of 3.5 kWp (3.3 kW inverter) cooperating with a two-axis tracking system and a cooling system produced 4.99 MWh in 12 months. This is a 5% increase in energy production compared to PV modules without a cooling system which produced 4.75 MWh. The cooling system works effectively in the summer months with high solar irradiance and ambient temperatures. In the research period, the cooling system increased the amount of energy produced by 236.1 kWh. Whereas, considering the four warmest months (June-September), the increase is equal to 180.6 kWh, which corresponds to a 7.3% increase in energy production.

The application of the two-axis tracking system (change of spatial orientation) and the cooling system (temperature coefficient of power γ) eliminated the most important factors causing reduced efficiency of the photovoltaic installation. The first solution tracks the apparent position of the Sun

on the celestial sphere which ensures appropriate incidence angle of solar radiation. The second solution reduces the influence of temperature coefficient of power PV module on its efficiency. The presented solutions can be merged a with solar concentrator system of a low concentration ratio (CR). The measurements, performed for *CR* equal to 1.5 and 2.0, showed that the cooling system kept the temperature of PV modules within the set range.

References

[1] Dupeyrat, P., Ménézo, C., & Fortuin, S. (2014). Study of the thermal and electrical performances of PVT solar hot water system. *Energy and Buildings*, *68*, 751–755. https://doi.org/10.1016/j.enbuild.2012.09.032

[2] Bayrak, F., Öztop, H. F., & Selimefendigil, F. (2020). Experimental study for the application of different cooling techniques in photovoltaic (PV) panels. *Energy Conversion and Management*, *212*, 112789. https://doi.org/10.1016/j.enconman.2020.112789

[3] Grubišić-Čabo, F., Nižetić, S., & Marco, T. G. (2016). Photovoltaic Panels: A review of the cooling techniques. *Transactions of Famena*, *40*(SI-1), 63–74. https://hrcak.srce.hr/file/234790

[4] Guarracino, I., Freeman, J., Ramos, A. C., Kalogirou, S. A., Ekins-Daukes, N. J., & Markides, C. N. (2019). Systematic testing of hybrid PV-thermal (PVT) solar collectors in steady-state and dynamic outdoor conditions. *Applied Energy*, *240*, 1014–1030. https://doi.org/10.1016/j.apenergy.2018.12.049

[5] Zondag, H. H. (2008). Flat-plate PV-Thermal collectors and systems: A review. *Renewable & Sustainable Energy Reviews*, *12*(4), 891–959. https://doi.org/10.1016/j.rser.2005.12.012

[6] Tiwari, G., Mishra, R. K., & Solanki, S. (2011). Photovoltaic modules and their applications: A review on thermal modelling. *Applied Energy*, *88*(7), 2287–2304. https://doi.org/10.1016/j.apenergy.2011.01.005

[7] Herrando, M., Pantaleo, A., & Markides, C. N. (2019). Solar combined cooling, heating and power systems based on hybrid PVT, PV or solar-thermal collectors for building applications. *Renewable Energy*, *143*, 637–647. https://doi.org/10.1016/j.renene.2019.05.004

[8] Vallati, A., Ocłoń, P., Colucci, C., Mauri, L., De Lieto Vollaro, R., & Taler, J. (2019). Energy analysis of a thermal system composed by a heat pump coupled with a PVT solar collector. *Energy*, *174*, 91–96. https://doi.org/10.1016/j.energy.2019.02.152

[9] Zaharil, H. A., & Hasanuzzaman, M. (2020). Modelling and performance analysis of parabolic trough solar concentrator for different heat transfer fluids under Malaysian condition. *Renewable Energy*, *149*, 22–41. https://doi.org/10.1016/j.renene.2019.12.032

[10] Tao, T., Zheng, H., He, K., & Mayere, A. (2011). A new trough solar concentrator and its performance analysis. *Solar Energy*, *85*(1), 198–207. https://doi.org/10.1016/j.solener.2010.08.017

[11] Aste, N., Tagliabue, L. C., Del Pero, C., Testa, D., & Fusco, R. (2015). Performance analysis of a large-area luminescent solar concentrator module. *Renewable Energy*, *76*, 330–337. https://doi.org/10.1016/j.renene.2014.11.026

[12] Mroczka, J., & Plachta, K. (2015, June). Modeling and analysis of the solar concentrator in photovoltaic systems. In *Modeling Aspects in Optical Metrology V* (Vol. 9526, pp. 340–347). SPIE. https://doi.org/10.1117/12.2184632

[13] Lan, J. (2023). Development and performance test of a novel solar tracking sensor. *Metrology and Measurement Systems*, *30*(2), 289–303. https://doi.org/10.24425/mms.2023.144870

[14] Arora, S., Singh, H., Sahota, L., Arora, M. K., Arya, R., Singh, S., Jain, A., & Singh, A. (2020). Performance and cost analysis of photovoltaic thermal (PVT)-compound parabolic concentrator (CPC) collector integrated solar still using CNT-water based nanofluids. *Desalination*, *495*, 114595. https://doi.org/10.1016/j.desal.2020.114595

[15] Imam, M. F. I. A., Beg, R. A., Rahman, M. L., & Khan, M. Z. H. (2016). Performance of PVT solar collector with compound parabolic concentrator and phase change materials. *Energy and Buildings*, *113*, 139–144. https://doi.org/10.1016/j.enbuild.2015.12.038

[16] Hanwha Q CELLS GmbH (2017). *Q.PEAK DUO-G8 345-360*.

[17] Walczak, M., Bychto, L., Kraśniewski, J., & Duer, S. (2022). Design and evaluation of a low-cost solar simulator and measurement system for low-power photovoltaic panels. *Metrology and Measurement Systems*, *29*(4), 685–700. https://doi.org/10.24425/mms.2022.143067

[18] Poulek, V., Matuška, T., Libra, M., Kachalouski, E., & Sedláček, J. (2018). Influence of increased temperature on energy production of roof integrated PV panels. *Energy and Buildings*, *166*, 418–425. https://doi.org/10.1016/j.enbuild.2018.01.063

[19] D'Orazio, M., Di Perna, C., & Di Giuseppe, E. (2014). Experimental operating cell temperature assessment of BIPV with different installation configurations on roofs under Mediterranean climate. *Renewable Energy*, *68*, 378–396. https://doi.org/10.1016/j.renene.2014.02.009

[20] Duffie, J. A., & Beckman, W. A. (1980). *Solutions Manual for Solar Engineering of Thermal Processes*. University of Wisconsin-Madison.

[21] Mesbahi, O., Tlemçani, M., Janeiro, F. M., Hajjaji, A., & Kandoussi, K. (2021). Sensitivity analysis of a new approach to photovoltaic parameters extraction based on the total least squares method. *Metrology and Measurement Systems*, *28*(4), 751–765. https://doi.org/10.24425/mms.2021.137707

[22] García, M. A., & Balenzategui, J. L. (2004). Estimation of photovoltaic module yearly temperature and performance based on Nominal Operation Cell Temperature calculations. *Renewable Energy*, *29*(12), 1997–2010. https://doi.org/10.1016/j.renene.2004.03.010

[23] Brihmat, F., & Mekhtoub, S. (2014, December). PV cell temperature/PV power output relationships homer methodology calculation. In *Conférence Internationale des Energies Renouvelables – CIER'13. International Journal of Scientific Research & Engineering Technology*, *1*(02).

[24] Plachta, K. (2020, April). Algorithm for precise positioning of photovoltaic panels. In *Photonics for Solar Energy Systems VIII* (Vol. 11366, pp. 65–70). SPIE. https://doi.org/10.1117/12.2557675

Kamil Płachta received Ph.D. degree from Wrocław University of Science and Technology, Poland. He has been a member of the teaching and research staff at the Department of Electronic and Photonic Metrology since 2013. His current research interests include renewable energy sources, mainly on systems that tracks the apparent position of the Sun on the celestial sphere.

Mariusz Ostrowski is lecturer of the Department of Electronic and Photonic Metrology at Wrocław University of Science and Technology, Poland. His research interests focus on renewable energy sources, mainly on systems for optimizing the generation and consumption of energy from PV panels.

Janusz Mroczka is a Professor at Wrocław University of Science and Technology, Poland, a founder of the Polish school of electronic and pho-tonic metrology, and a member of the Polish Academy of Sciences. He is director of the Department of Electronic and Pho-tonic Metrology at the Wrocław University of Science and Technology. His research interests include methodology of the cognitive process, algorithmisation of the inverse problem, indirect measurements badly conditioned numerically, methodology of combining measurement data with different spatial resolution using determin-istic and stochastic processing methods.